Progress in the analysis of the beta delayed proton and gamma decay of ^{27}P for nuclear astrophysics

E. Simmons,[1] L. Trache,[1] A. Banu,[1] A. Saastamoinen,[1,2] M. McCleskey,[1] B. Roeder,[1] A. Spiridon,[1] R.E. Tribble,[1] T. Davinson,[3] P. J. Woods,[3] G. J. Lotay,[3] J. Wallace,[3] and D. Doherty[3]

[1]*Cyclotron Institute, Texas A &M University, Texas, United Stated.*

[2]*If Department of Physics, University of Jyvaskyla, Finland*

[3]*School of Physics, University of Edinburgh, Edinburgh, United Kingdom*

Introduction & Astrophysical Motivation

When ^{26}Al is created in novae, the reaction chain is ^{24}Mg(p, γ)^{25}Al(β+ν)^{25}Mg(p, γ)^{26}Al, but this chain can be by-passed by another chain, ^{25}Al(p, γ)^{26}Si(p,γ)^{27}P, and ^{26}Al can also be destroyed. One interesting feature of ^{26}Al is that its ground state has a large spin $J^{\pi}=5^{+}$ and, only 228 keV above it there is an isomeric state with $J^{\pi}=0^{+}$, which also beta decays, but has a much shorter life time than the ground state. In stars these two states behave as 'different species' until temperatures go beyond 1GK, and then they are correlated. Now, one of the ways ^{26}Al can be destroyed is by ^{26m}Al(p,γ)^{27}Si*, which is dominated by resonant capture. This was the focus of one of our experiments.

Energetically speaking, stars are too cold to study their reaction rates directly, that is, the actual cross sections are too low to allow us to measure them easily in the lab. So, we need to apply an indirect method in order to gain the information we require. In the case of interest here (^{26}Al^{m}(p,γ)), the indirect method we chose to use was the study of beta-delayed gamma (βγ) and proton (βp) decay. As shown in Fig. 1, the direct method involves a proton tunneling through the Coulomb barrier of ^{26}Al^{m} to form

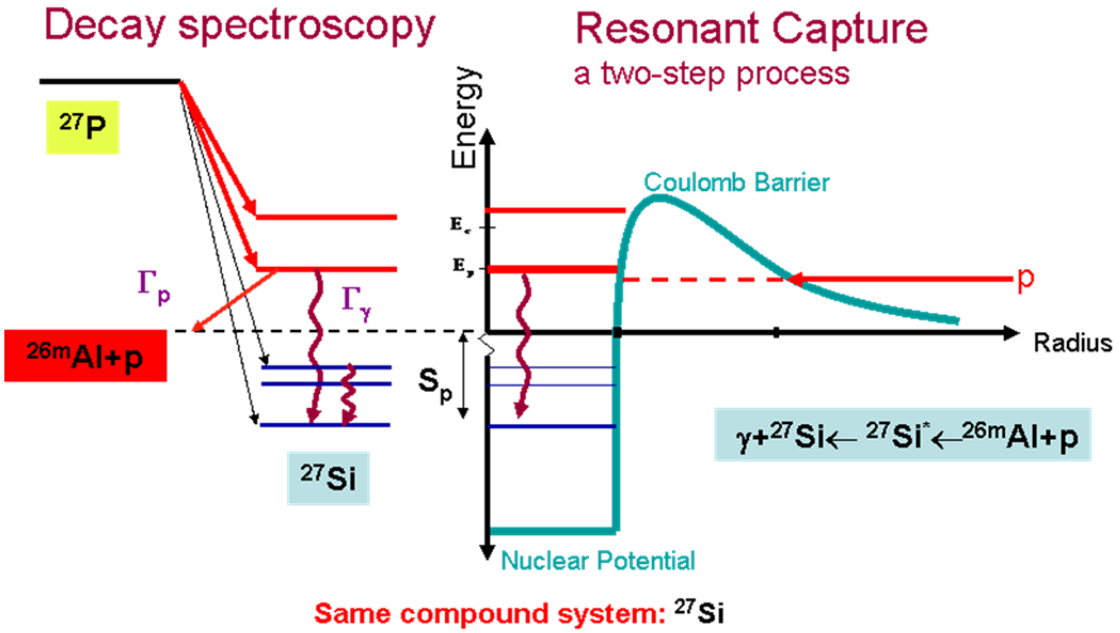

FIG. 1. Indirect method used to study resonances in the ^{26m}Al(p,γ) reaction. Note that they have the same compound system ^{27}Si.

excited states in ^{27}Si which then decay through gamma emission. Instead, starting with ^{27}P, it first β-decays to the same excited states in ^{27}Si (due to selection rules) and then decays through gamma emission. States populated above the proton threshold ($E^*>S_p + E(0^+) = 7.463 + 0.228 = 0.7661$ MeV) can decay by proton emission to $^{26}Al^m$ and these are the states of interest. In order to evaluate their contribution to the astrophysical reaction rate, we need to determine the position of the resonances and their partial gamma and proton widths.

Review of the Measurement

This experiment was run from Nov 24 to Dec 1 of 2010 using a primary beam of $^{28}Si^{+10}$ at 40 MeV/u obtained from the K500 superconducting cyclotron. A target of hydrogen gas, kept at LN_2 temps and 2 atm pressure, was used to create the desired ^{27}P by a (p, 2n) fusion evaporation reaction. After tuning and optimizing the secondary beam we ended up with about 11% total impurities, most of which was ^{24}Al.

The ^{27}P nuclei were implanted in the center of a thin detector where the decay occurred. A telescope combination of silicon detectors was used in this experiment. A thin (45 and later a 104 μm) double sided strip detector (DSSD), referred to here as the p-detector, was sandwiched between two thick (300 μm and 1 mm) silicon detectors, referred to as the β1 and β2 detectors respectively. The precise implantation in the middle of this very thin proton detector was possible due to the inherent high kinetic energy (30-40 MeV/u) of the exotic secondary beams produced using the in-flight technique and the good momentum control we have in MARS in combination with a rotating Al degrader foil, placed in front of the silicon detectors. By monitoring the two-dimensional histograms β1 vs Proton detector and the Proton detector vs β2 as the angle of the Al foil was changed, it was possible to see when the ^{27}P nuclei were implanted only in the center (proton) detector. This detector and degrader setup is shown below in Fig. 2.

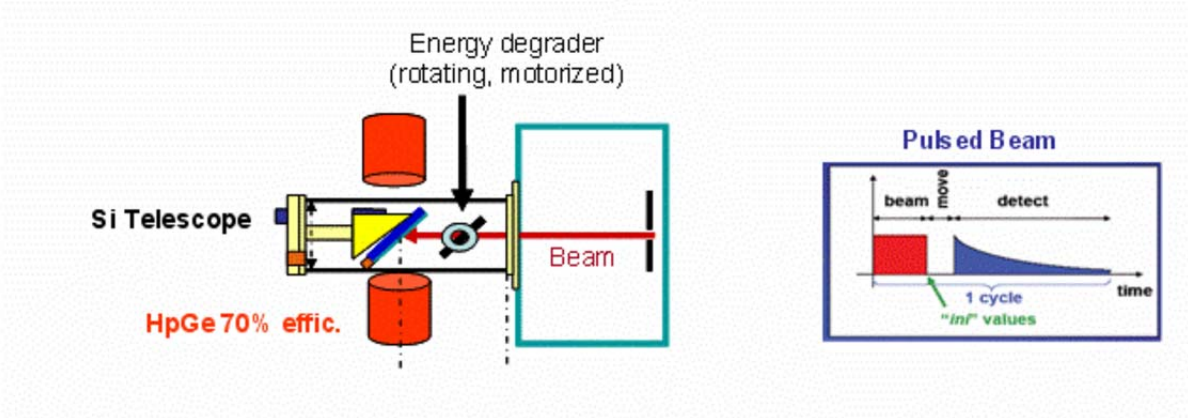

FIG. 2. Implantation and Decay Station Setup.

Using the β-detectors, p-detector and HpGe detectors, we measured, simultaneously, the β-p & β-γ coincidences. In order to do this the beam from the K500 cyclotron had to be pulsed, that is, ^{27}P was

implanted for a period of time, then the beam was switched off and the decay was measured before switching the beam back on and repeating the process.

Preliminary Results – Protons

The proton branching ratio for ^{27}P was known to be lower (0.07% total proton branching) compared to anything we had tried to measure before and was therefore, in many ways, a test run to see how far the β-background could be reduced. From preliminary analysis work it can be seen that, even through we were successful in substantially reducing the β-background from previous βp & βγ experiments, we still have a background issue in the low energy region of interest, which is made even more troublesome in this case due to the very low total proton branching ratio. These features can be seen below in Fig. 3.

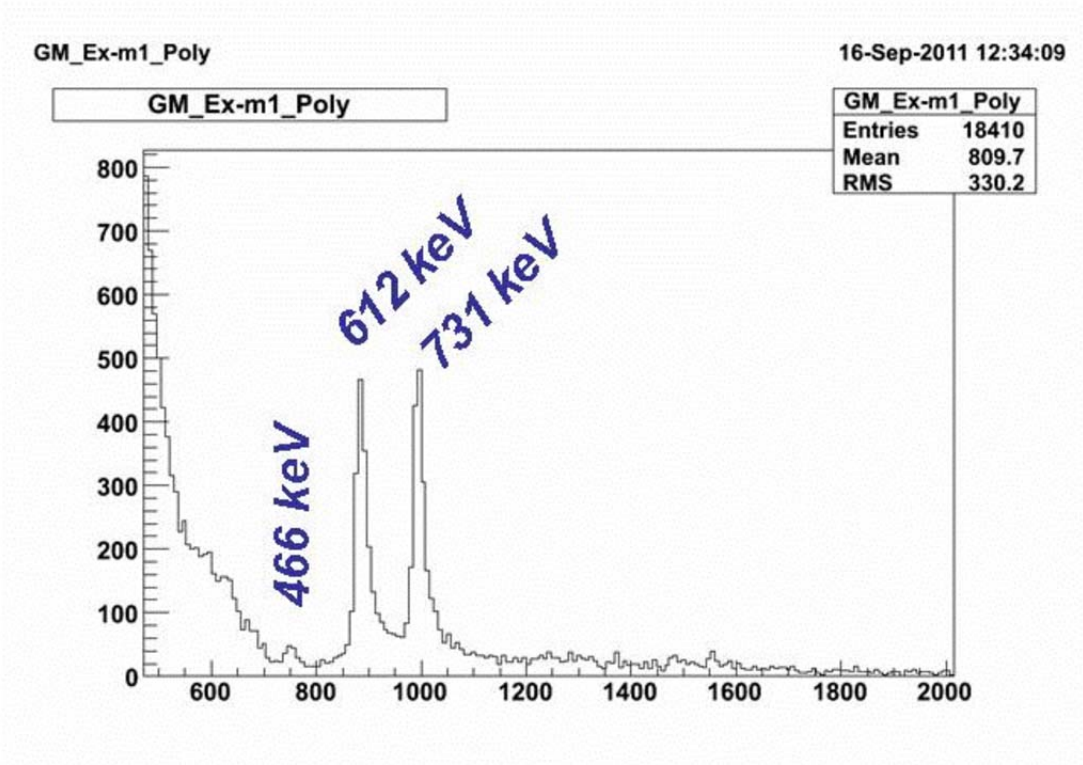

FIG. 3. Preliminary proton spectrum from the βp & βγ experiment. A BB2-45 detector was used for this data.

The higher energy protons, originally identified by the Berkeley group, are clearly seen here but, in the low energy region we saw mostly β's. As can be seen in Fig. 3, there is a clear structure above a continuous background in the low energy region 200 - 400 keV that suggests there is valuable information yet to be obtained**.** We have also determined that the total proton branching ratio is closer to 0.01% than the previous reported 0.07%.

Preliminary Results – Gammas

The gamma spectrum came out very nicely, especially in the high energy region, showing the pay off of having re-designed the implantation-decay station which allowed the HpGe's to be moved in as close as physically possible to the silicon detectors. The only impurities that were visible, due to our coincidence setup, came from impurities in the beam (^{22}Mg and ^{24}Al), see attached Fig 8. The ^{24}Al gammas were used, in addition to well known peaks identified in a background run, to create an extended energy calibration up to 8 MeV with residuals better than 2 keV for Germanium 1. It was found that the energy recoil had to be taken into account for the high energy gammas from ^{24}Al for the best calibration. Due to a non-linearity issue with Germanium 2, obtaining the best extended energy calibration requires using two separate fit ranges. That is, for energies up to about 1.7 MeV, one linear fit was used, and for energies 1.7 MeV to 8 MeV another linear fit was employed. Linear fits have so far proved slightly better than quadratic fits. Some work still needs to be done with these calibrations in order to get the residuals as good as Germanium 1. The current results for Germanium 2, with residuals for the major peaks, are shown below in Fig. 4.

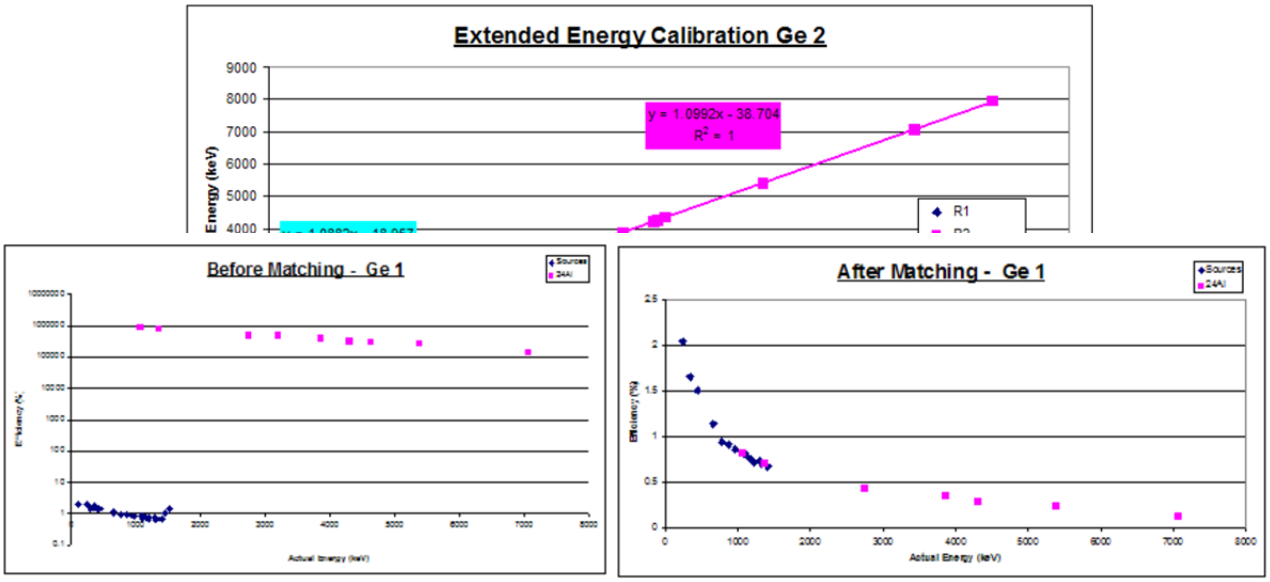

FIG. 5. Example of match ^{24}Al points to the efficiency curve created with the sources.

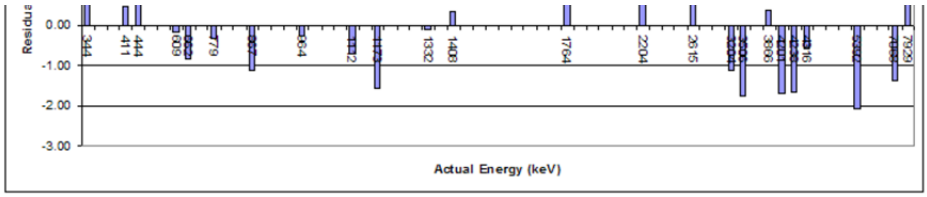

FIG. 4. Extended Energy Calibration for Germanium 2, showing the two ranges required.

An extended efficiency calibration was also obtained for each germanium detector using sources (^{152}Eu, ^{60}Co & ^{137}Cs) and the most intense peaks from ^{24}Al. This was done by first, using the source and

dead time information to create an efficiency calibration up to 1.4 MeV. Then, to include the ^{24}Al gammas, the sums (with background subtracted) divided by their absolute intensities were calculated for each peak, then, all of these values were multiplied by a common factor in order to match the efficiency points of the ^{24}Al to the curve created by the sources. This matching method is shown below in Fig. 5.

Further analysis at this point employed the use of the TAC data. Five TAC units were used to obtain information on the β_1-p (TAC 1), β_2-p (TAC 2), β_1-γ (TAC 3), β_2-γ (TAC 4) and the γ_1-γ_2 (TAC 5) coincidences. By carefully gating on the peaks that appear in these histograms it is possible to cut out some background (and reduce the impurities) without losing real information. Several different gating conditions are shown in Fig. 6. A spectrum was created when gates were placed on each individual relevant TAC (3, 4 and 5) and also with a combination of relevant TACs (3 OR 4 and 3 OR 4 OR 5). Note that the single TAC condition on TAC 3 (β_1-γ) has a larger reduction effect than TAC 4 (β_2-γ), pointing to the fact that the thicker β-detector (β_2) was more efficient, as expected.

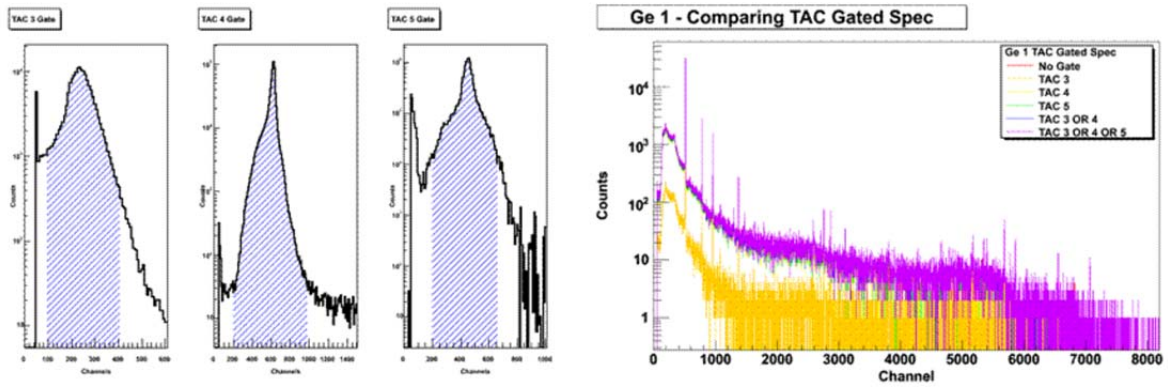

FIG. 6. TAC gates for the BB2-45 data on the left-hand side and various TAC-gated spectra on the right hand side.

The TAC-gated spectrum I will continue with at this point is the condition that an event corresponds within the (TAC 3 OR TAC 4 or TAC 5) gates. This spectrum is currently very similar to the original, non-TAC gated spectra, though it does seem to slightly reduce the impurities. Further analysis into these gates is needed to find the best results, that is, reducing the background as much as possible without compromising real counts.

The next step was to calculate the intensities of each gamma relative to the lowest gamma line (780 keV). First the background-subtracted sums have to be adjusted to take into account the efficiency of the detector. These numbers are then used to calculate the relative intensities. See equations below. Analysis of this is ongoing.

$$N_\gamma^i = \frac{A_\gamma^i}{\varepsilon(E_\gamma^i)} \pm \delta N_\gamma^i \qquad I_\gamma^i \equiv \frac{N_\gamma^i}{N_\gamma^1} \times 100$$

The results for the intensities of the major gammas are shown below in Table I in addition to the previously known values.

A preliminary decay scheme for these gamma lines is shown below in Fig 7. Many small peaks remain to be shorted out in order to determine if they are escape peaks or actual peaks, or maybe even a combination of the two cases. One method to help determine this is done by plotting the ratios for known cases where we have both the single escape (SE) and a double escape (SE) peak. That is, the ratio of the efficiency adjusted intensities of the SE to the original peak, and the DE to the original peak are plotted first, then, peaks that are suspected of being escape peaks are also plotted in this fashion (relative to their estimates original peaks). If the unknown points roughly follow the known points they are escape peaks, if they are very different, they are at least a combination of escape peaks and new peaks, if not entirely new peaks. Analysis on these data is currently ongoing.

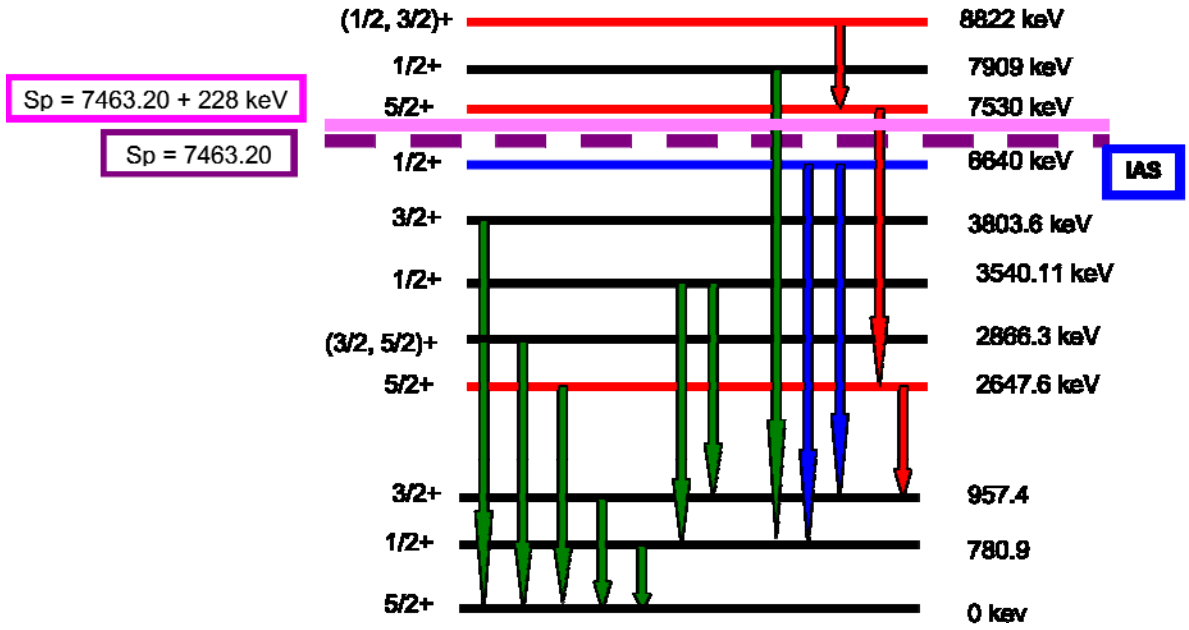

FIG. 7. Preliminary decay scheme for ^{27}Si. The blue lines come from the isobaric analog state, the green lines are the previously well known lines and the red are proposed new lines.

Future Plans

Future plans include finishing the analysis for the ^{27}P βp & βγ experiment and understanding the method and results from a lifetime experiment. This involves finalizing the decay scheme for the gammas, calculating the branching ratios and estimating the logft values. Using this information we may be able to say something new about the overall picture of ^{26}Al^{m} in nuclear astrophysics.

[1] K. Krane, *Introductory Nuclear Physics,* (John Wiley & Sons, Inc.,1988).

[2] D. Clayton, *Isotopes in the Cosmos*, (Cambridge University Press, 2003).

[3] J.A. Caggiano *et al*., Phys. Rev. C **64**, 025802 (2001).

[4] T.J. Ognibene *et al*., Phys. Rev C **54**, 1098 (1996).

[5] A. Saastamoinen, L. Trache *et al*., Phys. Rev. C **83**, 045808 (2011).

[6] L. Trache *et al*., Proc. 10th Symposium on Nuclei in the Cosmos (NIC X), Mackinac Island, Michigan, July 2008, PoS 163.